

# Physiological and Biodegradation Changes Properties of PLA\UHMWPE\PVA Blends During Early Stage of Biodegradation in Vivo

Enas al-Zubaidy<sup>1\*</sup>, Ahmed Fadhil Hamza<sup>1</sup>, Zuhair Jabbar Abdul Ameer<sup>2</sup>

<sup>1</sup>Department of Engineering of Polymer and Petrochemical Industries, College of Materials Engineering, University of Babylon, Hillah, Iraq

<sup>2</sup>Department of Prosthetics and Orthotics, College of Engineering, University of Karbala, Kerbala, Iraq

DOI: <https://doi.org/10.51244/IJRSI.2025.120800234>

Received: 23 August 2025; Accepted: 30 August 2025; Published: 30 September 2025

## ABSTRACT

Biodegradable plastic blends from natural sources, namely pure polylactic acid (PLA) and polyvinyl alcohol (PVA) with ultra-high molecular weight polyethylene (UHMWPE) softener, were studied to investigate changes in their physical properties resulting from in vivo biodegradation at body temperature. These blends are also suitable for the manufacture of medical scaffolds and artificial joints. Fourier transform infrared (FTIR) spectroscopy revealed a significant change in the chemical composition, manifested by improved cohesion and structural diffusion. Furthermore, a broad band appeared in the 3417–3471 cm<sup>-1</sup> region, representing a clear modification of the spectra and leading to the formation of a biofilm on the outer surface of the samples. DSC analysis supported the clear effect across all blend spectra. Changes in the gravimetric values confirmed that the PVA\PLA/UHMWPE samples degraded significantly faster with increasing PVA volume fraction, and PVA completely disappeared at higher volume fractions. It was also shown that PLA did not degrade rapidly into PLA/UHMWPE in vivo, maintaining its overall structure and weight unchanged.

**Keywords**—biodegradable PLA, biodegradable PVA, FTIR, in vivo

## INTRODUCTION

Poly lactic acid (PLA) is a biodegradable aliphatic polyester made from lactic acid (LA) or 2-hydroxypropionic acid, a thermoplastic polyester obtained from the polymerization of lactic acid and/or the ring-opening polymerization of lactide with the chemical formula (C<sub>3</sub>H<sub>4</sub>O<sub>2</sub>)<sub>n</sub>. PLA is produced by bacterial fermentation of carbohydrates from agricultural products such as corn, potatoes, and cassava [1]. The most important manufacturing methods, depending on the process, can be mentioned: injection molding, film extrusion, blow molding, thermoforming, fiber spinning, and film forming. PLA can be specially compounded for a specific application. The most important industries include: “packaging, textile, biomedical, structural, and automotive.” These industries are considered among the most important industries that use products derived from PLA [2]. PLA is biocompatible and has biodegradability, but some disadvantages have been reported in the literature, which include high cost, long-term degradability, and limited molecular weight [3]. Polyvinyl alcohol (PVA) is a colorless, odorless, water-soluble synthetic polymer with the molecular formula [CH<sub>2</sub>CH (OH)]<sub>n</sub>, obtained from the polymerization of vinyl acetate. It is widely used as a thickener in a variety of applications, including papermaking, sizing, packaging, and the medical and pharmaceutical industries[4]. PVA is the most important material in the photovoltaic solar cell industry due to its hydrophilic properties, chemical stability, and ability to form thin films. However, PVA has drawbacks, such as discrepancies between transmittance and selectivity. These problems have been addressed, however, by modifying PVA through chemical crosslinking, the use of fillers, blending with other materials, and doping[5]. UHMWPE is a polymer with mechanical and physical properties (excellent abrasion resistance, chemically inert, lubricability, biocompatible) [6], The mechanical and physical properties can be modified in the polymer synthesis process. Since UHMWPE is widely used in industrial and clinical applications. Currently,

approximately 2 million pathological conditions require implantation of artificial joints, and HMWPEU is used among the polymers every year[7]. Special requirements for UHMWPE to be applied in arthroplasty have been defined in ASTM F648 and ISO 5834-1. Compression molding and extrusion are two manufacturing processes widely performed to form bulk UHMWPE parts[8]. The polymer is produced using methods (compression molding and extrusion). Using the compression molding process, UHMWPE bars can be manufactured in a wide range of diameters. They are the most commercial polymer used for orthopedic purposes, and their diameters range from 20 to 80 mm [9]. Since UHMWPE has a high molecular weight and high viscosity even above its melting point, it is undoubtedly difficult to process by conventional screw extrusion[10]. After forming the UHMWPE block, the mechanical properties are modified to closely relate to the wear mechanisms using multiple methods.

The mechanical and physical properties of UHMWPE are affected by its crystallinity [11]. The effect of crystallization on the abrasion resistance of UHMWPE has been reported, and reported that as the percentage of crystallinity increases, the friction force and scratch depth decrease. Similar results have also been reported that the degree of crystallinity is increased by controlling the material formation pressure and temperature [12]. Sheets with a thickness of less than 12 nm were reported to be formed after heating UHMWPE (with a molecular weight of more than 400,000) under high pressure, followed by a back cooling process leading to the formation of the crystalline structure [13]. It has also been reported that when the temperature is held above the melting point (approximately 110 °C), the polyethylene chains can fold and thus crystalline sheets are formed with increasing crystallinity[14]. Using high-dose radiation to increase the hardness and improve the wear resistance of UHMWPE [15,16]. However, high radiation doses accelerate the oxidation process, which increases the failure of the material. Oxidation causes fragility and thus increases the rate of particulate wear of the bone component[10]. Therefore, vitamin E is added to improve the oxidation resistance, mechanical strength, and fatigue of cross-linked UHMWPE [17].

## MATERIALS AND METHODS

Circular samples of pure PLA, pure UHMWPE, pure PVA, (50% wt. PLA/ 50 % wt. UHMWPE) blends, were pressed into a mold with dimensions of (12 mm radius, 3 mm thickness, and total volume of 0.339 cm<sup>3</sup>) in a heat press at a temperature of 180 °C for 30 minutes. Then they were heat pressed under a pressure of 5 MPa. To investigate the decomposition of (PLA/UHMWPE) blends in vivo, the circular samples at the ratios (1:1), (1:2), and (1:3) were placed in a small plastic container containing a solution simulating body fluids, Fig. 1. These samples were removed and weighed using a sensitive balance before heating to 50°C.



**Fig. 1 PLA degradation**

They were weighed after heating, and the weights before and after burning were recorded from August 1, 2024, to the present, with no change in weight, as shown in Table I. For porous mixtures, PVA is used; the decomposition potential of PVA in water was revealed by placing circular samples prepared in the same way as above, but with the ratio as in Table II. The samples were placed in small cups containing water and with a

cloth-mesh, and left for 24 hours

**Table I Pla Degradation Measurement**

Before Heating		After Heating	
1:1	0.20 g	1:1	0.20 g
1:2	0.26 g	1:2	0.26 g
1:3	0.28 g	1:3	0.28 g

**TABLE II Specification of (PLA\UHMWPE\PVA) Blends**

Samples	PLA wt. %	UHMWPE wt. %	PVA wt. %
PLA\UHMWPE1	9	81	10
PLA\UHMWPE2	16	64	20
PLA\UHMWPE3	21	49	30
PLA\UHMWPE4	24	36	40
PLA\UHMWPE 5	25	25	50
PLA\UHMWPE 6	24	16	60
PLA\UHMWPE 7	21	9	70
PLA\UHMWPE 8	16	4	80
PLA\UHMWPE 9	9	1	90

## CHARACTERIZATION TECHNIQUES

### Fourier Transform Infrared Spectrometer (FTIR)

Fourier transform infrared spectroscopy (FTIR) is a technique used to distinguish between organic, inorganic, and polymeric groups present in materials according to ASTM E1252 standard. It was used to characterize the molecular structure of pure (PLA, UHMWPE, PVA), 50%PLA/ 50%UHMWPE, and 25% PLA/ 25% UHMWPE/ 50% PVA blends and interpret the bonds between the blends. The instrument used in this work is an IR Affinity-1 manufactured in Kyoto, Japan, and located in the Department of Polymer and Petrochemical Engineering, College of Materials Engineering, University of Babylon.

### Differential Scanning Calorimetry Test (DSC)

A differential calorimeter has been used to examine and quantify the temperature of the phase transitions of the samples of pure (PLA, UHMWPE, PVA), 50%PLA/ 50%UHMWPE, and 25% PLA/ 25% UHMWPE/ 50% PVA blends. The device used in this test is SHIMADZU-4 DSC-60, located in the Polymer Engineering and Petrochemical Industries Department / College of Materials Engineering / University of Babylon, and the test was performed under ASTM D3418-03 [19].

## RESULTS AND DISCUSSION

### FTIR Test Results and Discussion

Fig. (2, a), shows the vibrational absorption bands at ( $3757\text{ cm}^{-1}$ ) for PLA\UHMWPE, pure PLA, and pure UHMWPE, indicating the formation of O-H bonds. A large absorption band at ( $3471\text{--}3417\text{ cm}^{-1}$ ) was observed for PLA\UHMWPE, along with a small absorption band at ( $2924\text{ cm}^{-1}$ ) [18]. This is primarily due to hydroxyl groups and the (O-H stretching) vibration associated with carbohydrates. The peaks at ( $3039\text{--}2854\text{ cm}^{-1}$ ) are attributed to the CH group. This band showed higher absorption for PLA\UHMWPE compared to the pure spectrum, which is expected given that PLA leads to the formation of (-CH<sub>2</sub>- and -CH<sub>2</sub>- groups) [19]. For pure PLA, the carbonyl stretching absorption band was shown at ( $1774\text{ cm}^{-1}$ ), and this absorption appeared to be smaller in HMWPE\PLA. The increased absorption bands at the dimer ( $1720\text{--}1512\text{ cm}^{-1}$ ) are attributed to the formation of unsaturated (C=C bonds) in PLA\UHMWPE [20].

Similarly, for PLA at the dimer ( $1774\text{--}1504\text{ cm}^{-1}$ ), the peak was sharper and broader. An absorption peak was observed at ( $1658\text{ cm}^{-1}$ ) for PLA, and a smaller shift at ( $1620\text{ cm}^{-1}$ ) for PLA\UHMWPE. The presence of this peak indicates the transition of the polymer surface to one poor in hydrogen and rich in interconnected carbon atoms.

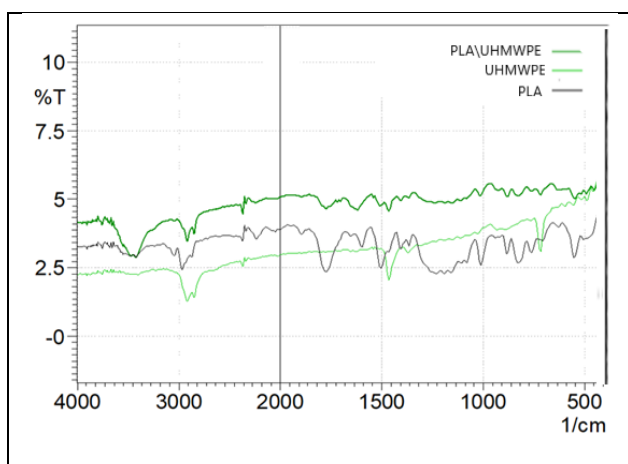
Furthermore, some carbonyl formation was observed at around ( $1720\text{ cm}^{-1}$ ) in the absorption spectrum of PLA\UHMWPE. Table III shows the main absorption areas of the spectrum (PLA\UHMWPE).

**TABLE III Absorption Areas of Fig. 2a**

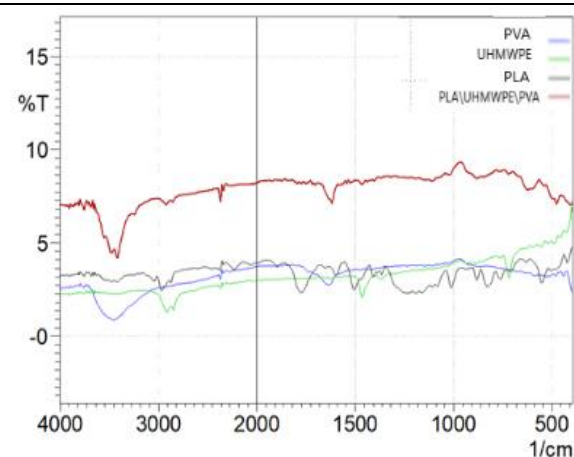
Type of bond	Pure PLA	Pure UHMWPE	PLA/UHMWPE
O - H Stretch	$3757\text{ cm}^{-1}$	$3757\text{ cm}^{-1}$	$3471 - 3417\text{ cm}^{-1}$
C - H Stretch	-	-	$2845 - 3039\text{ cm}^{-1}$
C = O stretch	$1774\text{ cm}^{-1}$	-	$1512\text{--}1658\text{ cm}^{-1}$

Vibrational absorption bands at  $1685\text{ cm}^{-1}$  were observed for the PLA\UHMWPE blend; the bands are more intense with their shift to a lower level, which is attributed to the interaction between PLA and UHMWPE, indicating the formation of C=O bonds.

Fig. (2, b), The C-H stretching bands for PLA\UHMWPE\PVA of formalin can be seen at the absorption peaks at ( $2924, 2845, 2762, \text{ and } 2677\text{ cm}^{-1}$ ) [21]. O-H stretching bands of PLA\UHMWPE\PVA are observed at ( $3500\text{ cm}^{-1}$ ) where the bands are more intense with shifting to a lower level. Ester bonds were observed at the band at ( $1620\text{ cm}^{-1}$ ) due to the (C-O bond), while the peaks at ( $1018\text{ and } 1111\text{ cm}^{-1}$ ) indicate the presence of (C-O bond). These bands can demonstrate the formation of ester bonds during the curing process [22]. It is expected that the C=O group in PLA will react with the O-H group in PVA to form hydrogen bonds. This reaction may improve the cohesion and diffusion between the three polymers without reacting with UHMWPE, Fig. 3. Table IV shows the main absorption areas of the spectrum (PLA\UHMWPE\PVA).



(a) The spectrum of (PLA\UHMWPE)



(b) The spectrum of (PLA\UHMWPE\PVA)

fig. 2 FTIR microscopic for blends

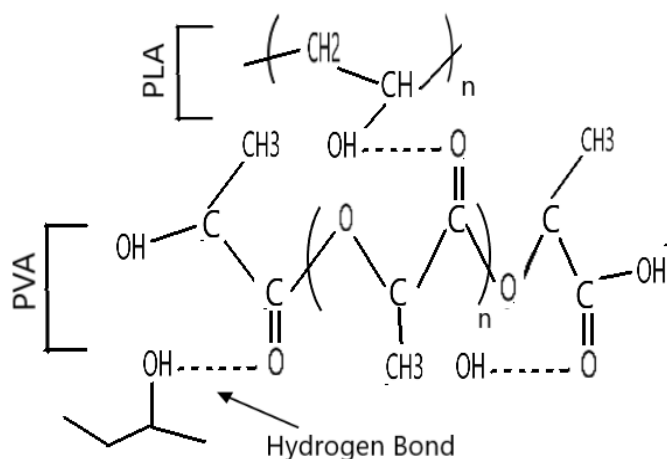


Fig. 3 The reaction of PFGBs constituents (porous layer)

TABLE IV Absorption Areas of Fig. 2b

Type of bond	Pure PLA	Pure UHMWPE	Pure PVA	PLA/UHMWPE\PVA
O - H Stretch	3448 cm <sup>-1</sup>	3417 cm <sup>-1</sup>	3500 - 3700 cm <sup>-1</sup>	3500 cm <sup>-1</sup>
C - H Stretch	-	-	-	2677-2762-2845-2924 cm <sup>-1</sup>
C - O Stretch	1111-1018 cm <sup>-1</sup>	-	-	1620 cm <sup>-1</sup>
C = O stretch	1650 cm <sup>-1</sup>	-	1400 cm <sup>-1</sup>	1400 cm <sup>-1</sup>

## PVA Degradation Results and Discussion

After the samples were placed in small cups containing water, covered with a cloth-mesh for 24 hours. It was observed that the samples from (PLA/UHMWPE/PVA 1...PLA/UHMWPE /PVA 5) did not decompose significantly, some of which decomposed partially. In contrast to the samples from (PLA/UHMWPE/PVA



6...PLA/UHMWPE/ PVA 9), some of which decomposed completely, as shown in Fig. 4. The sample (PLA/UHMWPE/PVA 5) is partially decomposed then similarly the blends are etched and are more suitable for medical scaffolds and artificial joints such as the trunk and knee as an outer layer that helps in bone integration and tissue exchange.

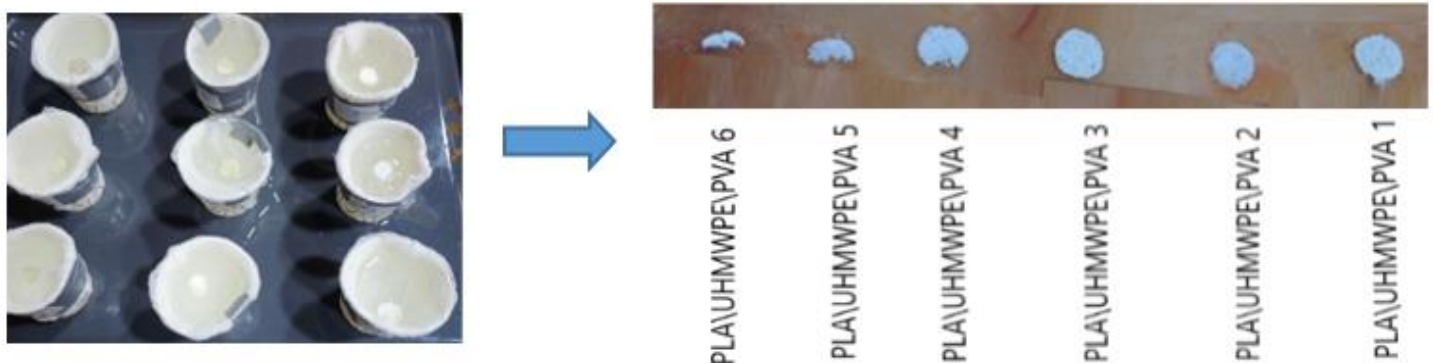
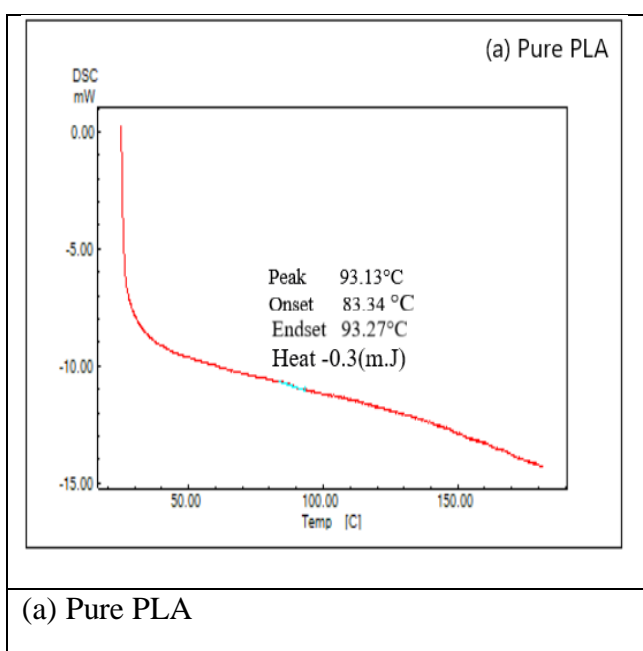


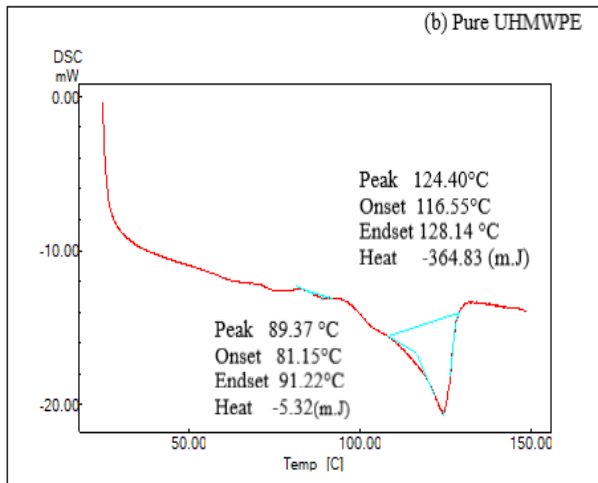
**Fig. 4 PVA degradation**

### Differential Scanning Calorimetry Results (DSC)

Although FTIR data reveal the chemical "family" of the polymer in question, identifying the polymer subclass often requires additional analytical methods. One useful and rapid method is to perform a dynamic differential scanning calorimetry (DSC) thermogram of the polymer to determine its thermal transitions. DSC is a technique for measuring the total heat flow into and out of a material as a function of temperature and/or time. Therefore, all thermal phenomena within a mixture can be measured by DSC. Fig. (5, a), for example, shows a conventional DSC result (total heat flow) for pure PLA polymer. Only one transition can be observed at 93.13 °C as received. For Fig. (5, b) pure UHMWPE, two transitions are observed: the glass transition at 89.37 °C and the crystal melting at 124.40 °C. Fig. (5, c) the PLA/UHMWPE polymer blend exhibits two transitions: the glass transition at 73.37°C and the crystalline melt at 127.19°C. This is attributed to the flexible phase of UHMWPE, which increases the polymer's ability to evaporate water. It also increases heat flow upon heating and passing through the glass transition, with the crystalline temperature and melting point decreasing with increasing fill percentage.

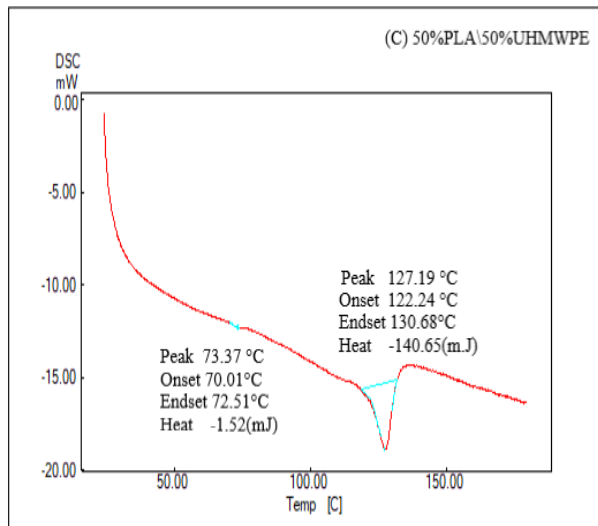


(b) Pure UHMWPE



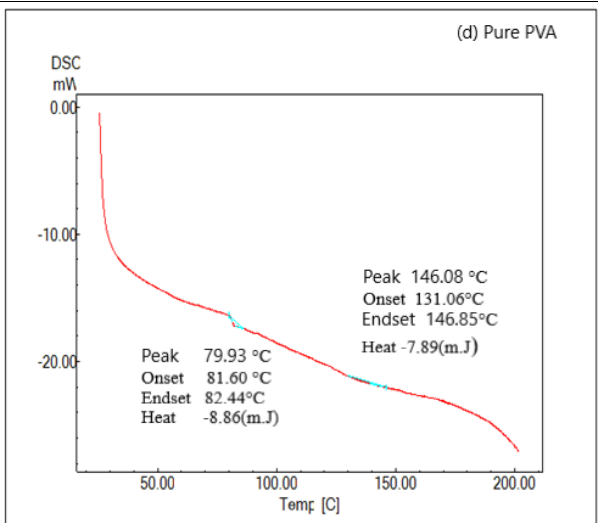
(b) Pure UHMWPE

(C) 50%PLA\50%UHMWPE



(c) PLA\UHMWPE

(d) Pure PVA



(d) Pure PVA

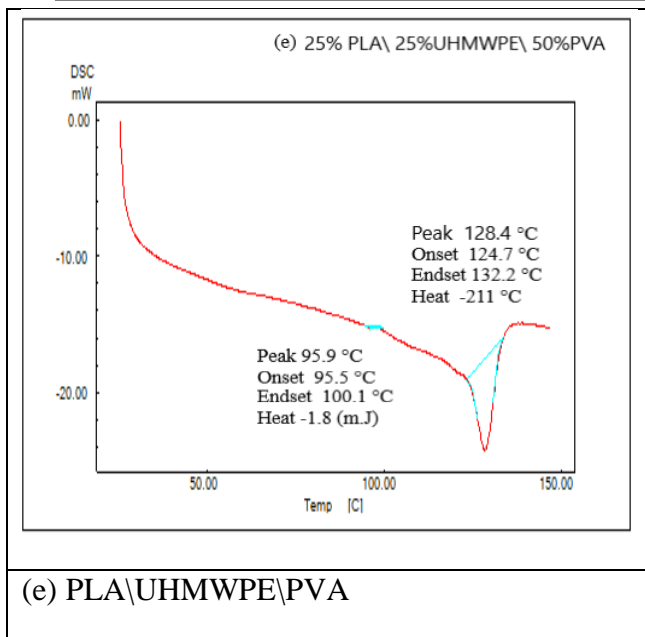


**Fig. 5 DSC results**

Fig. (5, c) The melting point of 50%PLA/ 50%UHMWPE was observed to be elevated to 127.19 °C. Similarly, the estimated degree of crystallinity decreased to 73.37 °C. When HMWPE is blended into a PLA matrix, distinct crystalline regions are formed, resulting in a higher  $T_m$  due to the additional thermal stability provided by the UHMWPE crystalline domains. Furthermore, the interaction of the two polymers at the molecular level plays a very important role. Thus, hydrogen bonding patterns and phase separation significantly contribute to the thermal properties [23]. Studies have confirmed that during DSC heating cycles, increased molecular interactions between phases hinder the mobility of PLA chains and cause the temperature to drop upwards, at which point the energy required to overcome the covalent interactions between polymers becomes very high. Recently, new phase change materials have been exported [24–27] or characterized for use in phase change [28, 29].

Fig. (5, d) shows a glass transition at 79.93°C, as well as a second glass transition (at 146.08°C). Polyvinyl alcohol (PVA) is a semi-crystalline polymer, meaning it contains both amorphous (random) and crystalline (ordered) regions.  $T_g$  1 corresponds to the glass transition occurring in the amorphous regions, where the polymer chains gain kinetic energy and become rubbery.  $T_g$  2, if observed at a higher temperature, corresponds to the crystalline melting regions within the PVA structure [30].

In Fig. (5, e), the melting point of UHMWPE/PLA/PVA was observed to rise to 128.4 °C. Similarly, the estimated degree of crystallinity increased to 95.9 °C. A similar result was observed for the PVA/PLA blend, but with a large displacement and a higher  $T_g$  values were observed, which also indicates good miscibility of PVA into the PLA and UHMWPE phases. A new phase. The observed increase in phase volume for this sample also supports the occurrence of miscibility.

## CONCLUSION

Current research into the biodegradability and physiological effects of composites may be beneficial from both scientific and practical perspectives. Under these conditions, a reasonable biodegradation rate is required for years, which is the majority of which contains poly lactic acid. Furthermore, the biodegradability of polyvinyl alcohol is beneficial for medical applications. The most important findings are:

Poly lactic acid in combination with ultra-high molecular weight polyethylene is beneficial for biomaterial applications and is the closest match to human bone.

The results of polyvinyl alcohol biodegradation are exciting for the production of composites that achieve osseointegration and biotransformation in vivo.



The PVA/PLA/UHMWPE composites exhibit effective hydrogen bonding, which improves cohesion and diffusion between the three polymers.

The PLA/UHMWPE spectrum represents a clear modification of the pure spectra and leads to the formation of a biofilm on the outer surface of the samples at (3417–3471  $\text{cm}^{-1}$ ).

## REFERENCES

- Kandemir, N., Yemenicioglu, A., Mecitoglu, Ç., Elmaci, Z. S., Arslanoglu, A., Göksungur, Y., & Baysal, T. (2005). Production of antimicrobial films by incorporation of partially purified lysozyme into biodegradable films of crude exopolysaccharides obtained from *Aureobasidium pullulans* fermentation. *Food Technology and Biotechnology*, 43(4), 343-350.
- Ilyas, R. A., Sapuan, S. M., Harussani, M. M., Hakimi, M. Y. A. Y., Haziq, M. Z. M., Atikah, M. S. N., ... & Asrofi, M. (2021). Polylactic acid (PLA) biocomposite: Processing, additive manufacturing and advanced applications. *Polymers*, 13(8), 1326.
- Castro-Aguirre, E., Iniguez-Franco, F., Samsudin, H. E. A., Fang, X., & Auras, R. (2016). Poly (lactic acid)—Mass production, processing, industrial applications, and end of life. *Advanced drug delivery reviews*, 107, 333-366.
- Nagarkar, R., & Patel, J. (2019). Polyvinyl alcohol: a comprehensive study. *Acta Sci. Pharm. Sci*, 3(4), 34-44.
- Halake, K., Birajdar, M., Kim, B. S., Bae, H., Lee, C., Kim, Y. J., ... & Lee, J. (2014). Recent application developments of water-soluble synthetic polymers. *Journal of Industrial and Engineering Chemistry*, 20(6), 3913-3918.
- Zhang, H. X., Shin, Y. J., Lee, D. H., & Yoon, K. B. (2011). Preparation of ultra high molecular weight polyethylene with  $\text{MgCl}_2/\text{TiCl}_4$  catalyst: Effect of internal and external donor on molecular weight and molecular weight distribution. *Polymer bulletin*, 66(5), 627-635.
- Kurtz, S. M. (Ed.). (2009). UHMWPE biomaterials handbook: ultra high molecular weight polyethylene in total joint replacement and medical devices. Academic press.
- Walter, W. L., Walter, W. K., & O'Sullivan, M. (2004). The pumping of fluid in cementless cups with holes. *The Journal of arthroplasty*, 19(2), 230-234.
- Kurtz, S. M. (2009). From ethylene gas to UHMWPE component: The process of producing orthopedic implants. In *UHMWPE biomaterials handbook* (pp. 7-19). Academic Press.
- Lim, K. L. K., Ishak, Z. M., Ishaku, U. S., Fuad, A. M. Y., Yusof, A. H., Czigany, T., ... & Ogunniyi, D. S. (2005). High-density polyethylene/ultrahigh-molecular-weight polyethylene blend. I. The processing, thermal, and mechanical properties. *Journal of Applied Polymer Science*, 97(1), 413-425.
- Karupiah, K. K., Bruck, A. L., Sundararajan, S., Wang, J., Lin, Z., Xu, Z. H., & Li, X. (2008). Friction and wear behavior of ultra-high molecular weight polyethylene as a function of polymer crystallinity. *Acta Biomaterialia*, 4(5), 1401-1410.
- Wang, S., & Ge, S. (2007). The mechanical property and tribological behavior of UHMWPE: Effect of molding pressure. *Wear*, 263(7-12), 949-956.
- Oral, E., Christensen, S. D., Malhi, A. S., Wannomae, K. K., & Muratoglu, O. K. (2006). Wear resistance and mechanical properties of highly cross-linked, ultrahigh-molecular weight polyethylene doped with vitamin E. *The Journal of arthroplasty*, 21(4), 580-591.
- Medel, F. J., & Puértolas, J. A. (2008). Wear resistance of highly cross-linked and remelted polyethylenes after ion implantation and accelerated ageing. *Proceedings of the Institution of Mechanical Engineers, Part H: Journal of Engineering in Medicine*, 222(6), 877-885.
- Oral, E., Beckos, C. A. G., Lozynsky, A. J., Malhi, A. S., & Muratoglu, O. K. (2009). Improved resistance to wear and fatigue fracture in high pressure crystallized vitamin E-containing ultra-high molecular weight polyethylene. *Biomaterials*, 30(10), 1870-1880.
- Jahan, M. S. (2016). ESR insights into macroradicals in UHMWPE. In *UHMWPE biomaterials handbook* (pp. 668-692). William Andrew Publishing.
- Bracco, P., & Oral, E. (2011). Vitamin E-stabilized UHMWPE for total joint implants: A review. *Clinical Orthopaedics and Related Research*, 469(8), 2286-2293.
- Maizatun, N., Norazowa, I., Yunus, W. M. Z. W., Khalina, A., & Khalisanni, K. (2013). FTIR and TGA analysis of biodegradable poly (lactic acid)/treated kenaf bast fibre: Effect of plasticizers. *Pertan. J. Sci.*

Technol, 21, 151-160.

19. Wunderlich, B. (2012). *Macromolecular physics* (Vol. 2). New York, NY: Academic Press.
20. Valenza, A., Visco, A. M., Torrisi, L., & Campo, N. (2004). Characterization of ultra-high-molecular-weight polyethylene (UHMWPE) modified by ion implantation. *polymer*, 45(5), 1707-1715.
21. Morais, M. S., Bonfim, D. P., Aguiar, M. L., & Oliveira, W. P. (2023). Electrospun poly (vinyl alcohol) nanofibrous mat loaded with green propolis extract, chitosan and nystatin as an innovative wound dressing material. *Journal of Pharmaceutical Innovation*, 18(2), 704-718.
22. Thomas, L. V., Arun, U., Remya, S., & Nair, P. D. (2009). A biodegradable and biocompatible PVA–citric acid polyester with potential applications as matrix for vascular tissue engineering. *Journal of Materials Science: Materials in Medicine*, 20(Suppl 1), 259-269.
23. Corradini, E., Mattoso, L. H. C., Guedes, C. G. F., & Rosa, D. S. (2004). Mechanical, thermal and morphological properties of poly ( $\epsilon$ -caprolactone)/zein blends. *Polymers for advanced technologies*, 15(6), 340-345.
24. Chen, Z. H., Yu, F., Zeng, X. R., & Zhang, Z. G. (2012). Preparation, characterization and thermal properties of nanocapsules containing phase change material n-dodecanol by miniemulsion polymerization with polymerizable emulsifier. *Applied Energy*, 91(1), 7-12.
25. Cai, Y., Ke, H., Dong, J., Wei, Q., Lin, J., Zhao, Y., ... & Fong, H. (2011). Effects of nano-SiO<sub>2</sub> on morphology, thermal energy storage, thermal stability, and combustion properties of electrospun lauric acid/PET ultrafine composite fibers as form-stable phase change materials. *Applied Energy*, 88(6), 2106-2112.
26. Wang, L., & Meng, D. (2010). Fatty acid eutectic/polymethyl methacrylate composite as form-stable phase change material for thermal energy storage. *Applied Energy*, 87(8), 2660-2665.
27. Darkwa, J., Su, O., & Zhou, T. (2012). Development of non-deform micro-encapsulated phase change energy storage tablets. *Applied Energy*, 98, 441-447.
28. Li, M., Wu, Z., & Kao, H. (2011). Study on preparation, structure and thermal energy storage property of capric–palmitic acid/attapulgate composite phase change materials. *Applied energy*, 88(9), 3125-3132.
29. Zhang, Z., Zhang, N., Peng, J., Fang, X., Gao, X., & Fang, Y. (2012). Preparation and thermal energy storage properties of paraffin/expanded graphite composite phase change material. *Applied Energy*, 91(1), 426-431.
30. Haines, P. J., Reading, M., & Wilburn, F. W. (1998). Differential thermal analysis and differential scanning calorimetry. In *Handbook of thermal analysis and calorimetry* (Vol. 1, pp. 279-361). Elsevier Science BV.